

A lattice Boltzmann study of non-hydrodynamic effects in shell models of turbulence

R. Benzi¹, L. Biferale^{1*}, M. Sbragaglia¹,
S. Succi² and F. Toschi²

¹ Dipartimento di Fisica and INFN, Università "Tor Vergata",
Via della Ricerca Scientifica 1, I-00133 Roma, Italy

² Istituto per le Applicazioni del Calcolo, CNR,
Viale del Policlinico 137, I-00161, Roma, Italy

February 8, 2008

Abstract

A lattice Boltzmann scheme simulating the dynamics of shell models of turbulence is developed. The influence of high order kinetic modes (ghosts) on the dissipative properties of turbulence dynamics is studied. It is analytically found that when ghost fields relax on the same time scale as the hydrodynamic ones, their major effect is a net enhancement of the fluid viscosity. The bare fluid viscosity is recovered by letting ghost fields evolve on a much longer time scale. Analytical results are borne out by high-resolution numerical simulations. These simulations indicate that the hydrodynamic manifold is very robust towards large fluctuations of non hydrodynamic fields. *Key words: Turbulence, Kinetic Theory, Lattice Boltzmann, Shell Models.*

1 Introduction

In the recent years it has been speculated that modern developments in (discrete) kinetic theory might yield a new angle of attack to the problem of turbulence modeling [1, 2]. The rationale behind this idea is as follows. All turbulence models based on the Navier-Stokes hydrodynamic equations

*Corresponding author: L.Biferale, Dept. of Physics, University of Tor Vergata, Via della Ricerca Scientifica 1, 00133 Rome, ph +390672594595; email:biferale@roma2.infn.it

work on the assumption of a scale separation between the resolved and unresolved eddies [4, 5, 6]. By resolved eddies, we mean excitations at a scale larger than the grid size of the simulation. Such an assumption is never satisfied in turbulent flows, particularly close to solid boundaries, where turbulence production and removal are strongly unbalanced. This is the reason why all eddy-viscosity models fail to reproduce accurately turbulent statistics in strongly non-homogeneous situations. Kinetic theory is at a vantage point to describe such strongly out of equilibrium conditions, since it does not require any scale separation between the 'fast' and 'slow' degrees of freedom. We wish to emphasize that we are referring to an *effective* kinetic theory dealing with the dynamics of *quasiparticles*, i.e. effective degrees of freedom of the turbulent flow [20, 21, 22].

In any eddy-viscosity model the effect of small eddies on the large ones results in a typical diffusion process, only with a much enhanced turbulent diffusivity. In contrast to eddy-viscosity, the kinetic approach is centered upon the more general and fundamental notion of *relaxation*, controlled usually by a single characteristic time, τ entering in the Boltzmann equation. The ratio between the relaxation time and the typical hydrodynamical time, τ_h , is called the Knudsen number, $Kn = \tau/\tau_h$. In the limit of small Kn , the Boltzmann equation converges to the Navier-Stokes equations [20, 23]. The major question is: how to derive a suitable effective kinetic Boltzmann equation for the dynamics of large scale in turbulent flows? In principle, such an equation should be derived ab-initio through a renormalization-group procedure, starting from the true Boltzmann equation for molecules. Preliminary attempts in this ambitious direction look very encouraging, and yet not conclusive [7]. While waiting for a rigorous derivation, a practical strategy is to resort to discrete versions of the Boltzmann equation, now known as Lattice Boltzmann equation (LBE), and endow it with a self-consistent relaxation operator [8]. The crucial asset of LBE is that it provides a minimal form of kinetic theory compatible with the physics of turbulent flows, and such that it can be simulated very efficiently on present-day computers. This approach, sometimes called LBE- τ , has been recently shown to provide leading-edge numerical results for turbulent flows in real-life geometries [8]. Despite the impressive results, these simulations leave many theoretical ends open, and 'whether a theory can be developed remains to be seen' [9]. Leaving aside the important issue of numerical efficiency, from a purely theoretical perspective, a relevant question is whether the added value of the kinetic approach to fluid turbulence can be linked to the the dynamics of non-hydrodynamic fields, high order kinetic moments of the Boltzmann distribution, sometimes called ghost fields [10, 11, 12, 13]. Ghost fields represent the hidden kinetic information which, although necessary to guarantee the correct local symmetries, does not normally emerge to the macroscopic scale. In this

paper we aim at investigating the role of the dynamics of ghost fields in the kinetic approach to fluid turbulence. In particular, we focus our attention on the effects of ghost fields on the small-scale statistics of high Reynolds number flows. Unfortunately, due to limitations in computational power, it is still impossible nowadays to perform numerical simulation in the fully developed turbulent regime. To reach high Reynolds numbers flows, with a clear separation between the energy injection and the energy dissipation scales, one needs to resort to some model of turbulence. A popular class of deterministic dynamical models, widely used in recent years, is given by “shell-models” [14]. Shell models represent the only example where flows at high Reynolds numbers, with realistic small-scales statistics, can be studied. They are a good test-bed for new theories and numerical schemes aimed at improving the understanding of small-scales turbulent behaviour. The paper is organized as follows. First we propose a Lattice Boltzmann scheme for shell-models. Second, we study analytically and numerically its hydrodynamical limit with particular emphasis on the importance of ghosts fields for the small scales dynamics. Finally, we present numerical and analytical results on the “multi-relaxation” regime, i.e. the case when hydrodynamic fields and ghost fields have two different relaxation properties to the local equilibrium.

2 Shell models

Shell models are the simplest dynamical systems featuring a realistic picture of energy transfer from large to small scales [15, 14]. The main advantage of shell models is that they can be analyzed in great depth via highly accurate numerical simulations, which permit to resolve up to six decades in momentum space. They are non-linear deterministic models of Navier-Stokes equations, built such as to preserve energy, helicity and phase-space volume in the inviscid and unforced limit. In this work we shall focus on the following shell model [16]:

$$\partial_t U_n = ik_n Q_n - \nu k_n^2 U_n + F_n \quad (1)$$

where the non linear term is given by:

$$Q_n = U_{n-2}^* U_{n-1} + \frac{b}{2} U_{n-1}^* U_{n+1} + \frac{(1+b)}{4} U_{n+1} U_{n+2}. \quad (2)$$

In the above U_n is a complex variable representing the fluctuating velocity field at wavenumber $k_n = 2^n k_0$, and b is a free parameter fixing the physical dimension of the second inviscid invariant (here we fixed $b = -0.5$). In the presence of a large-scale forcing $F_n = F \delta_{n,0}$, this model exhibits

excellent scaling laws, from many aspects indistinguishable from those of real turbulence. For example, the p -th order structure functions

$$S_p(n) = \langle |U_n|^p \rangle \sim k_n^{-\zeta(p)} \quad (3)$$

are characterized by a set of scaling exponents, $\zeta(p)$, very close to those measured on turbulent flows. Many other aspects, connected to the velocity probability density functions, energy dissipation statistics and multi-time multi-scale correlation functions are also in good agreement with what measured in experimental and numerical studies of Navier-Stokes equations. For these reasons shell models have represented a unique occasion to investigate small-scale turbulent statistics without the difficulties of the original Navier-Stokes equations. Despite their apparent simplicity, a full systematic analytical control of the small-scale statistical behaviour is still lacking. Recently, a series of promising closure attempts based on stochastic closures have been proposed [17, 18, 19]. Yet, they cannot be considered conclusive. The importance of Lattice Boltzmann schemes for the shell-model (2) is therefore twofold. First, they may shed some lights on the complex multi-time dynamics of the hydrodynamical limit, second they may be useful to control, and optimize, convergence to the hydrodynamic limit, which may be useful also for LB schemes of Navier-Stokes equations.

3 LBE shell model

In this section we shall develop a discrete kinetic model whose hydrodynamic limit is precisely the shell model eq.(2). To this purpose we introduce a 5-speed lattice Boltzmann scheme in the wave number space, k_n , obeying the following dynamic equations:

$$\partial_t f_j(k_n) + ik_n f_j(k_n) = -\frac{1}{\tau} (f_j(k_n) - f_j^{eq}(k_n)) \quad (4)$$

where $f_j = [f_0, f_1, f_2, f_3, f_4]$ is the discrete distribution associated to the discrete speeds $c_j = [0, 1, -1, 2, -2]$. The local equilibrium is given by

$$f_j^{eq}(k_n) = w_j [R_n + c_j U_n + (c_j^2 - 1) D_n] \quad (5)$$

where $w_j = [6/12, 2/12, 2/12, 1/12, 1/12]$ are normalized weights. The equivalent of the macroscopic density and velocity fields are defined as follows:

$$R_n = \sum_{j=0}^4 f_j(k_n) \quad U_n = \sum_{j=0}^4 f_j(k_n) c_j. \quad (6)$$

The third macroscopic field, the analogue of the traceless momentum flux tensor, must be adjusted in such a way as to reproduce the non-linear term

Q_n in the shell model. After simple algebra, one derives:

$$2D_n + R_n = Q_n. \quad (7)$$

Let us notice that the shell-model equations we want to mimick are written in terms of a complex variable, U_n . Therefore, here the $f_j(k_n)$'s loose the nature of probability density functions they usually have in LB schemes in real space (complex distribution functions have been already used in the past to simulate quantum mechanics [24, 25]).

The first consequence is that in order to keep the “macroscopic density” for shell n , R_n , constant in time, one has to modify the streaming term in (4) for rest particles as follows:

$$\partial_t f_0(k_n) = -ik_n(2f_3(k_n) - 2f_4(k_n) + f_1(k_n) - f_2(k_n)) - \frac{1}{\tau}(f_0(k_n) - f_0^{eq}(k_n)) \quad (8)$$

By a linear transformation, we move to the momenta representation for the stress tensor, $S_n = \sum_j f_j(k_n)c_j^2$, and two ghost fields, $A_n = f_4(k_n) - f_3(k_n)$ and $B_n = f_3(k_n) + f_4(k_n)$. The resulting equations are:

$$\partial_t R_n = 0 \quad (9)$$

$$\partial_t U_n = ik_n S_n \quad (10)$$

$$\partial_t S_n = ik_n U_n + 6ik_n A_n - \frac{1}{\tau}(S_n - Q_n) \quad (11)$$

$$\partial_t A_n = 2ik_n B_n - \frac{1}{\tau}(A_n - \frac{1}{3}U_n) \quad (12)$$

$$\partial_t B_n = 2ik_n A_n - \frac{1}{\tau}(B_n - \frac{1}{4}Q_n) \quad (13)$$

The set of equations (9-13) is our kinetic shell model. From the first three equations, we obtain

$$\partial_t U_n + \tau \partial_{tt} U_n = ik_n Q_n - \tau k_n^2 U_n - 6\tau k_n^2 A_n. \quad (14)$$

This is the master equation of our treatment. First of all, we inspect its hydrodynamic limit. To this purpose, we notice that in the limit $\tau \rightarrow 0$ the ghost field A_n collapses onto its attractor, the velocity field:

$$\lim_{\tau \rightarrow 0} A_n = \frac{U_n}{3} \quad (15)$$

so that (14) delivers:

$$\partial_t U_n = ik_n Q_n - 3\tau k_n^2 U_n - \tau \partial_{tt} U_n. \quad (16)$$

It is therefore seen that, upon neglecting the term $\tau \partial_{tt} U_n$, which is indeed higher order in the Knudsen number, the correct shell model is reproduced in the limit $Kn \rightarrow 0$, with the ghost field contributing a factor 2τ to the flow viscosity. A perturbative expansion in τ of all fields appearing in (14), reveals that the effect of ghost fields at second order in Kn , yields a non-conservative contribution of the form

$$\tau^2 k_n^3 Q_n. \quad (17)$$

The finite-Knudsen regime is therefore characterized by the interplay of *three* distinct terms, namely:

$$k_n Q_n \quad (\text{inertial term}) \quad (18)$$

$$\tau k_n^2 U_n \quad (\text{dissipative term}) \quad (19)$$

$$\tau^2 k_n^3 Q_n \quad (\text{ghost contribution}). \quad (20)$$

Dimensional matching of these competing terms delivers the relevant crossover scales in Fourier space:

- Dissipative scale (Dissipation=Inertia):

$$k_d \sim \frac{1}{\tau^{3/4}} \quad (21)$$

- Ghost scale (Ghost term=Inertia):

$$k_g \sim \frac{1}{\tau}. \quad (22)$$

These relations show that $k_g \sim \frac{k_d}{\tau^{1/4}} \gg k_d$ for $\tau \ll 1$ which means that the ghost fields cannot play any role on the dissipation properties of the system since they do not reach up to the dissipative scale. In order to elicit a non-trivial role for the ghost fields, we need to realize the condition $k_g < k_d$. This necessarily leads to a generalized LBE in which ghost fields relax on their own timescale, longer than the hydrodynamic one. The minimal such choice is to define *two* relaxation times: τ_ν and τ_g , for hydrodynamic and ghost fields respectively. Since we aim at a fully turbulent regime, we shall consider for τ_ν the smallest possible values compatible with grid resolution. The relaxation time for the ghost field will then be changed in order to investigate its effects on the dissipation properties of the system.

4 Multi-relaxation shell BGK model

The simplest multi-relaxation kinetic shell model takes the following two-time form:

$$\partial_t R_n = 0 \quad (23)$$

$$\partial_t U_n = ik_n S_n \quad (24)$$

$$\partial_t S_n = ik_n U_n + 6ik_n A_n - \frac{1}{\tau_\nu}(S_n - Q_n) \quad (25)$$

$$\partial_t A_n = 2ik_n B_n - \frac{1}{\tau_g}(A_n - \frac{1}{3}U_n) \quad (26)$$

$$\partial_t B_n = 2ik_n A_n - \frac{1}{\tau_g}(B_n - \frac{1}{4}Q_n). \quad (27)$$

This set of equations is easily reproduced by going back to earliest LB formulations, in which collisional effects were taken into account through a scattering matrix M_{ji} describing the interaction between the j -th and i -th populations:

$$\partial_t f_j(k_n) + ik_n f_j(k_n) = M_{ji}(f_i(k_n) - f_i^{eq}(k_n)). \quad (28)$$

Following the top-down procedure introduced in [26], we can construct a scattering matrix with eigenvalues $\lambda = \{0, 0, -1/\tau_\nu, -1/\tau_g, -1/\tau_g\}$ and a corresponding set of kinetic eigenvectors, $V_j^{(k)}$, $k = 0, 4$, associated with the set of fields R_n, U_n, S_n, A_n, B_n , respectively:

$$f_j(k_n) = R_n V_j^{(0)} + U_n V_j^{(1)} + S_n V_j^{(2)} + A_n V_j^{(3)} + B_n V_j^{(4)}.$$

This corresponds to a partition of the five-dimensional kinetic space into a hierarchy of two conserved quantities (R_n, U_n), one quasi-conserved (transport) quantity (S_n) and two ghost fields (A_n, B_n). Using (24) and (25) we obtain:

$$\partial_t U_n = ik_n Q_n - \tau_\nu k_n^2 U_n - 6\tau_\nu k_n^2 A_n - \tau_\nu \partial_{tt} U_n. \quad (29)$$

where the dependence on τ_g is implicitly hidden within the fields A_n and U_n . It is worth pointing out that at this stage we are still dealing with *exact* equations. In order to get a first guess on the dynamics of ghost fields in this case, we make the approximation of imposing steady-state conditions on the ghost fields equations (26,27):

$$0 = 2ik_n B_n - \frac{1}{\tau_g}(A_n - \frac{1}{3}U_n) \quad (30)$$

$$0 = 2ik_n A_n - \frac{1}{\tau_g}(B_n - \frac{1}{4}Q_n). \quad (31)$$

This yields:

$$A_n = \frac{U_n}{3P(k_n\tau_g)} + \frac{ik_n\tau_g Q_n}{2P(k_n\tau_g)}, \quad P(k_n\tau_g) = 1 + 4k_n^2\tau_g^2. \quad (32)$$

This steady-state approximation must be understood as an estimate for the mean value of the fields. We show later, by direct numerical simulations of the eqs. (23-27), that the prediction extracted out of (30) and (31), yields the correct qualitative and quantitative statistical behaviours. It is also quickly checked that in the limit $\tau_g = \tau_\nu \ll 1$ the relation (32) reduces to the expression (15), as it should. For further analysis it proves convenient to explore the behaviour of (32) in the two regimes of small and large scales separately.

4.1 Large scales

Setting $\tau_g = 1$, large scales are identified by the condition $k_n \ll 1$. In this regime, the denominator of (32) simplifies, $P(k_n\tau_g) \rightarrow 1$, and we obtain:

$$-6\tau_\nu k_n^2 A_n \approx -3ik_n^3 \tau_g \tau_\nu Q_n - 2\tau_\nu k_n^2 U_n \quad (33)$$

Upon substituting this in the master equation (29) we get:

$$\partial_t U_n = ik_n Q_n (1 - 3ik_n^2 \tau_g \tau_\nu) - 3\tau_\nu k_n^2 U_n - \tau_\nu \partial_{tt} U_n. \quad (34)$$

It is therefore apparent that, since $\tau_\nu \ll \tau_g = 1$ and $k_n \ll 1$, the relative correction to the convective term, $3\tau_g \tau_\nu k_n^2$, is negligible. As a result, we come to the conclusion that the large-scale regime is virtually uncontaminated by the ghost fields.

4.2 Small scales

Small scales are identified by the condition $k_n \gg 1$, again with the position $\tau_g = 1$. In this regime the denominator $P(k_n\tau_g)$ is dominated by the k_n^2 term, so that the master equation delivers:

$$-6\tau_\nu k_n^2 A_n \approx -3ik_n \frac{\tau_\nu}{\tau_g} Q_n - \frac{2\tau_\nu}{\tau_g^2} U_n \quad (35)$$

Upon substituting in (29), we obtain

$$\partial_t U_n = ik_n (1 - \frac{\tau_\nu}{\tau_g}) Q_n - \tau_\nu k_n^2 U_n - \frac{2\tau_\nu}{\tau_g^2} U_n - \tau \partial_{tt} U_n. \quad (36)$$

From this expression we notice that the renormalized convective term is still conservative, with a renormalized factor $1 - \tau_\nu/\tau_g \sim 1$. The viscous

term becomes $-\tau_\nu k_n^2 U_n$, corresponding to a viscosity $\nu = \tau_\nu$, i.e. three times lower than in the previous case. Apart from the usual second order time derivative of the velocity field, the remaining piece, $-2\tau_\nu/\tau_g^2 U_n$, is a sub-leading damping term, due to the combined effect of high wavenumbers and long ghost relaxation time. In other words, ghosts can act at scales larger than the dissipative scale, but their amplitude is suppressed by a factor τ_ν/τ_g and consequently they gently disappear from the scene, leaving the system with the bare ghost-free viscosity τ_ν . Summarizing, the present analysis leads to the following predictions:

- Hydrodynamic scenario: $\tau_g = \tau_\nu \ll 1$, ghost fields are enslaved to their local equilibrium values. They contribute an extra term $2\tau_\nu$ to the fluid viscosity and do not affect the convective terms to any appreciable extent. At small but finite Knudsen numbers they are confined to sub-dissipative scales only and cannot produce any further appreciable effect. As a result, the correct hydrodynamic limit is recovered, with an enhanced viscosity $\nu = 3\tau_\nu$.
- Non-hydrodynamic scenario: $\tau_\nu \rightarrow 0, \tau_g = 1$, ghost fields are no longer enslaved to the fluid velocity. They receive contributions from the velocity field and the non-linear term Q_n at *all* scales through the propagator $P(k_n \tau_g)$. As a result, they exhibit high-frequency, small-amplitude fluctuations, which do not affect the large scale behavior of the system because they are suppressed by a τ_ν/τ_g factor. The correct hydrodynamic limit is still recovered, with a bare viscosity three times smaller than in the the previous case, $\nu_0 = \tau_\nu$.

5 Numerical results

The theoretical scenario discussed in the previous section has been tested against numerical simulations of the kinetic shell model. As a first test, we have simulated the kinetic shell model in the hydrodynamic regime, namely $\tau_\nu = \tau_g = 5 \times 10^{-4}$, with $k_n = 2^{n-13}$, $n = 1, 25$. For the sake of a quantitative comparison, the same simulations have been repeated with the original shell model (1) (with a viscosity $\nu = 3\tau_\nu$). In Figure 1 we show the energy spectra for the two cases. An excellent agreement between the LB and the shell model simulations is observed across the *whole* range of scales, except for scales well inside the dissipative range. In the inset of figure (1) we also present a check of the enslaving relation (15) by plotting the ratio between the ghost field and the velocity field, $3Re(A_n)/Re(U_n)$ for two typical wavenumbers, at large scales, $n = 6$ and at small scales close to the dissipative cut-off, $n = 18$. Notice how the relation (15) is perfectly verified at large scales, while some, small, deviation from slaving is observed at the

end of the inertial range. This confirms our theoretical analysis, namely that ghost fields are completely enslaved to their equilibrium values and do not affect the hydrodynamic behaviour of the turbulent system. Only strongly dissipative physics is affected by the ghost dynamics. The global stability is not changed.

More interesting, is to explore numerically the non-hydrodynamic regime, $\tau_g \sim O(1)$. We have performed a set of simulations with, $\tau_\nu = 5 \times 10^{-4}$, $\tau_g \sim O(1)$. The corresponding spectra for the velocity field are shown in Figure 2, where the case $\tau_\nu = \tau_g$ is also reported to highlight the effect of the reduced viscosity from $\nu = 3\tau_\nu$ to $\nu_0 = \tau_\nu$. As predicted by our theoretical analysis, the LB model in the non-hydrodynamic regime reproduces turbulent shell dynamics with the correct hydrodynamic viscosity $\nu_0 = \tau_\nu$ while the ghost field tends to decrease in intensity by going to smaller and smaller scales. Now ghosts are decoupled from the velocity fluctuations and the enslaving relation (15) is no longer satisfied. Still, they do not have any significant impact on the dynamics of the velocity field because their intensity is negligible (see inset of Figure 2).

A deeper insight into the role of ghost fields at all scales, inertial and dissipative, can be gained by inspecting the structure functions (3). In particular, in figure 3 we show the fourth and sixth order flatness $F_n^{(4)} = \frac{\langle U_n^4 \rangle}{\langle U_n^2 \rangle^2}$ and $F_n^{(6)} = \frac{\langle U_n^6 \rangle}{\langle U_n^2 \rangle^3}$ as a function of n for the hydrodynamic and non-hydrodynamic regime. The shell-model results are also presented. First we observe that both quantities have a clear dependency on the scale, that is a sign of intermittency in the velocity statistics. Second, all numerical results agree in the two regimes, the only difference being an increased inertial range extension when ghosts fields decouple.

6 Conclusions

Summarizing, we have presented a detailed analysis of the effects of non-hydrodynamic (ghost) fields on the statistical properties of hydrodynamic turbulence, within the framework of shell models. As a first result, we have shown that if ghost fields relax on the same time-scale as the hydrodynamic one, $\tau_g = \tau_\nu$ (the common scenario in current real-space LB simulations), then in the hydrodynamic limit where this scale is sent to zero, the ghost fields contribute to the hydrodynamic viscosity with a ratio 2 : 1 with respect to the weight of the hydrodynamic fields: $\nu = 2\tau_g + \tau_\nu$. Higher order ghost contributions, at finite relaxation times, are segregated to sub-dissipative scales, so that no further effects on the hydrodynamic behaviour can result. The non-hydrodynamic 'overtake' scenario ($k_g < k_d$) can be realized by allowing ghost fields a longer lifetime than hydrody-

dynamic modes. It is then found that ghost fields do *not* spoil the inertial physics (large scales) up to a negligible correction τ_ν/τ_g . The dissipative properties of the turbulent system are also reproduced, but now without the ghost contribution, leading to an hydrodynamic bare viscosity smaller than in the previous case: $\nu_0 = \tau_\nu$.

Our analysis supports the counter-intuitive notion that letting ghosts 'alive' on long time scales leads to a reduction of the viscosity, as compared to the case in which ghosts are frozen to their hydrodynamic equilibria.

Once extrapolated to the framework of real-space lattice Boltzmann models, our findings provide a motivation towards multirelaxation models, as opposed to the currently popular single-time relaxation BGK model. This come-back of multirelaxation models has been invoked by other groups as well [27], based on motivations of improved (linear) stability.

It is tempting to speculate that real-space LB simulations of two and three-dimensional turbulence might profit by moving (back) to a multi-relaxation scenario in which the hydrodynamic scale is kept to its minimum fixed by grid resolution, while the ghost fields time-scale is made much longer.

On a similar vein, one may speculate that making the hydrodynamic and ghost time scales respond self-consistently to turbulence observables, but with distinct functional dependencies, may prove beneficial also for LBGK- τ simulations with turbulence modeling [8]. As a final remark, our results provide a clear evidence that the hydrodynamic manifold is very robust against large fluctuations of non-hydrodynamic fields.

7 Acknowledgments

Illuminating discussions with S. Ansumali, H. Chen, I. Karlin, S. Orszag and V. Yakhot are kindly acknowledged.

References

- [1] H. Chen, S. Succi, S. Orszag, *Phys. Rev. E* **59**, R2527, (1999).
- [2] S. Succi, O. Filippova, H. Chen, S. Orszag, *J. Stat. Phys* **107**, 261, (2002).
- [3] S. Succi, I. Karlin, H. Chen, S. Orszag, *Physica A* **280**, 92, (2000).
- [4] C. Meneveau and J. Katz, *Annu. Rev. Fluid Mech.* **32**, 1, (2000).
- [5] Geurts, M. (2004): *Elements of direct and large-eddy simulation*, R.T. Edwards Inc..

- [6] Lesieur, M. and Metais, O. (1994): *Ann. Rev. Fluid Mech.* **28**, 45–82.
- [7] S. Ansumali, I.V. Karlin, and S. Succi, *Kinetic theory of turbulence modeling: Smallness parameter, scaling and microscopic derivation of Smagorinsky model*, LANL cond-mat/0310618, (2003), to appear in *Physica A*.
- [8] H. Chen, S. Kandasamy, S. Orszag, R. Shock, S. Succi, and V. Yakhot, *Science* **301**, 633–636, (2003).
- [9] R. Benzi, *Getting a grip on turbulence*, *Science* **301**, 605–606, (2003).
- [10] R. Benzi, S. Succi, M. Vergassola, *Phys. Rep.* **222**, 145, (1992);
- [11] M. Vergassola, R. Benzi, S. Succi, *Europhys. Lett.* **13**, 411, (1990);
- [12] P. Dellar, *Phys. Rev. E* **65**, 036309, (2002);
- [13] D. A. Wolf-Gladrow, “Lattice-Gas Cellular Automata and Lattice Boltzmann Models”, *Lecture Notes in Mathematics*, 1725, Springer (Berlin), 2000.
- [14] L. Biferale, *Ann. Rev. Fluid Mech.* **35** 441, (2003).
- [15] U. Frisch, *Turbulence, The legacy of A. Kolmogorov*, Cambridge Univ. Press, (1996).
- [16] V. S. L’Vov, E. Podivilov, A. Pomyalov, I. Procaccia, D. Vandembroucq, *Phys. Rev. E* **58** 1811, (1996).
- [17] R. Benzi, L. Biferale, F. Toschi, *J. Stat. Phys.* **113** 738, (2003).
- [18] R. Benzi, L. Biferale, M. Sbragaglia, F. Toschi, *Phys. Rev. E* **68** 046304, (2003).
- [19] R. Benzi, L. Biferale, M. Sbragaglia, *J. Stat. Phys.* **114** 137, (2004).
- [20] C. Cercignani, *Theory and application of the Boltzmann equation*, *Elsevier*, New York, (1975).
- [21] G. McNamara, G. Zanetti, *Phys. Rev. Lett.* **61**, 2332, (1988);
- [22] P. Bhatnagar, E. Gross, M. Krook, *Phys. Rev. A* **94**, 511, (1954).
- [23] Y. Qian, D. d’Humières, P. Lallemand, *Europhys. Lett.* **17**, 479, (1992).
- [24] S. Succi, R. Benzi, *Physica D* **69**, 327, (1993).
- [25] S. Succi, *The Lattice Boltzmann Equation for Fluid Dynamics and Beyond*, Oxford University Press, (2001);

- [26] F. Higuera, S. Succi, R. Benzi, *Europhys. Lett.* **9**, 345, (1989);
- [27] P. Lallemand, L.S. Luo, *Phys. Rev. E* **61**, 6546, (2000);

FIGURE 1

Comparison between the original shell model and our LB model. We plot $\log_2 \langle |U_n|^2 \rangle$ vs n for the shell model with viscosity $\nu = 3\tau_\nu$ (+) and the LB kinetic model with $\tau_\nu = \tau_g = 5 \times 10^{-4}$ (\times). Both models have the same forcing acting on the first two shells. Inset: check of the ghost-velocity slaving in the hydrodynamic regime. We plot $Re(3A_n(t))/Re(U_n(t))$ vs t for shell index $n = 6$ (straight line) and $n = 18$ (dotted line) with $\tau_\nu = \tau_g = 5 \times 10^{-4}$. Notice the small deviation observed at the smallest scale.

FIGURE 2

Velocity spectra for hydrodynamic and non-hydrodynamic LB regime. We plot $\log_2 \langle |U_n|^2 \rangle$ vs n for the LB model with the following choice of parameters: $\tau_\nu = \tau_g = 5 \times 10^{-4}$ (+) and $\tau_\nu = 5 \times 10^{-4}$, $\tau_g = 1$ (\times). Notice the increase of the inertial-range extension in the multi-relaxation LB model because the ghost field (\star) is completely negligible at small scales. Inset: check of the ghost-velocity slaving in the non-hydrodynamic regime. We plot $Re(3A_n(t))/Re(U_n(t))$ vs t for shell index $n = 6$ (straight line) and $n = 18$ (dotted line) with $\tau_g = 1$. Notice now, at difference from the case of fig. 1, that the velocity and the ghost fields at small scales are decoupled, being the overall intensity of the ghost field negligible.

FIGURE 3

Analysis of the flatness $F_n^{(p)} = \langle U_n^p \rangle / \langle U_n^2 \rangle^{p/2}$ for different values of p . We plot $\log_2 F_n^{(4)}$ vs n in our kinetic model for the following choice of parameters: $\tau_\nu = \tau_g = 5 \times 10^{-4}$ (\times) and $\tau_\nu = 5 \times 10^{-4}$, $\tau_g = 1$ (+); to emphasize the correct behaviour of the system we also plot the same quantity in the case of the original shell model with viscosity $\nu_0 = \tau_\nu$ (\star). Inset: the same cases but for the sixth order flatness $F_n^{(6)} = \langle U_n^6 \rangle / \langle U_n^2 \rangle^3$.

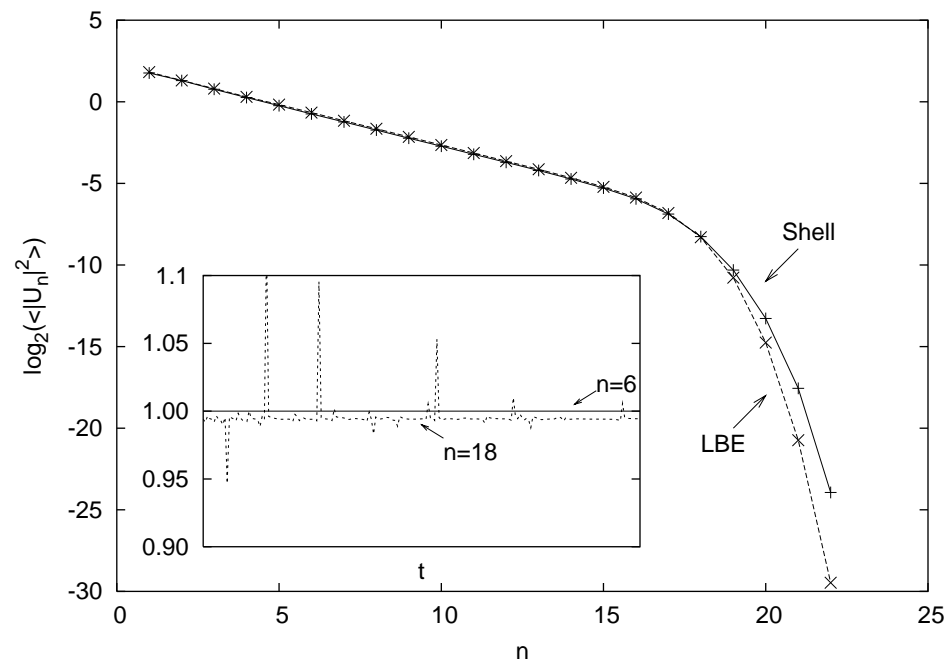


Figure 1:

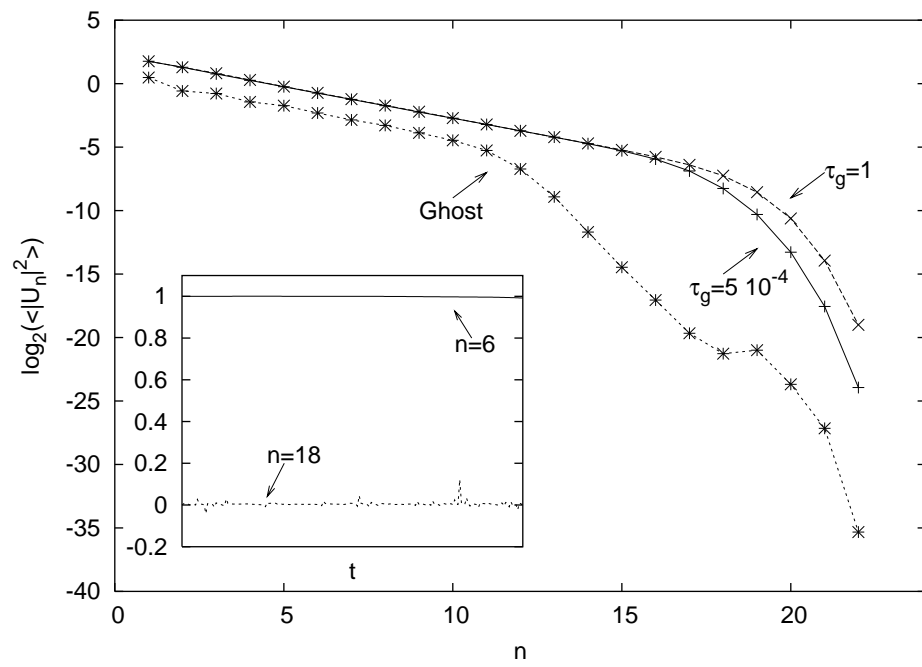


Figure 2:

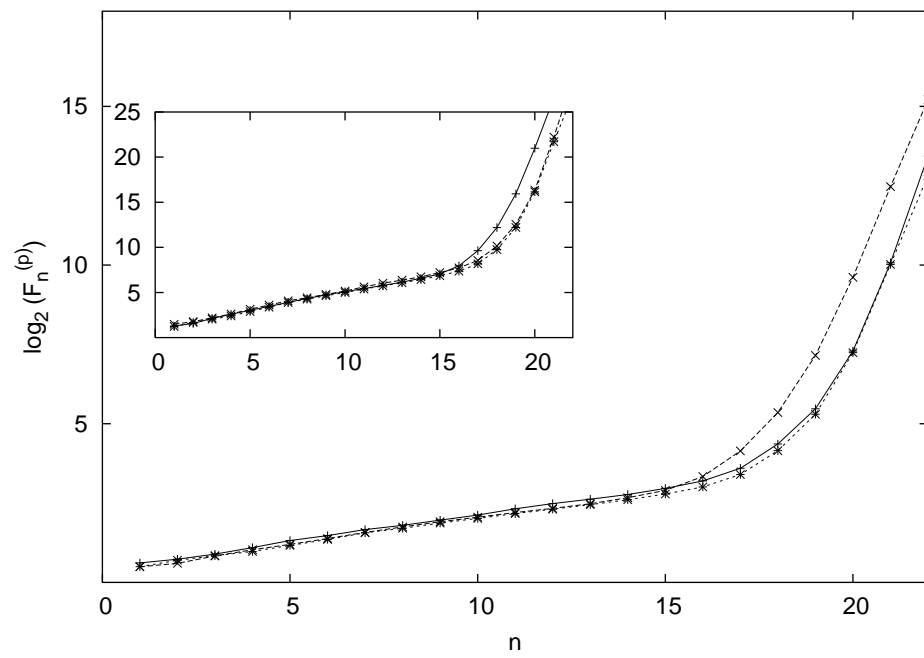


Figure 3: